



Title 論文題目	AMP deaminase in the ER-mitochondria interface promotes mitochondrial Ca ²⁺ overload in type 2 diabetic rat hearts. 2型糖尿病ラットにおいて、小胞体-ミトコンドリア接触領域に局在するAMPデアミナーゼはミトコンドリアCa ²⁺ 過負荷を促進する
Author(s) 著者	長南, 新太
Degree number 学位記番号	甲第3214号
Degree name 学位の種別	博士(医学)
Issue Date 学位取得年月日	2023-03-31
Original Article 原著論文	J Diabetes Investig. 2023 Apr;14(4):560-569
Doc URL	
DOI	10.1111/jdi.13982
Resource Version	Publisher Version

AMP deaminase in the ER-mitochondria interface promotes mitochondrial Ca²⁺ overload in type 2 diabetic rat hearts

Arata Osanami¹, Tatsuya Sato^{1,2}, Yuki Toda¹, Masaki Shimizu¹, Atsushi Kuno^{1,3}, Hidemichi Kouzu¹, Toshiyuki Yano¹, Wataru Ohwada¹, Toshifumi Ogawa¹, Tetsuji Miura^{1,4} and Masaya Tanno^{1*}

¹Department of Cardiovascular, Renal and Metabolic Medicine, Sapporo Medical University School of Medicine, Sapporo, Japan

²Department of Cellular Physiology and Signal Transduction, Sapporo Medical University School of Medicine, Sapporo, Japan

³Department of Pharmacology, Sapporo Medical University School of Medicine, Sapporo, Japan

⁴Department of Clinical Pharmacology, Faculty of Pharmaceutical Sciences, Hokkaido University of Science, Sapporo Japan

Keywords

AMP deaminase, Diabetic cardiomyopathy, Mitochondria-associated ER membrane

*Correspondence

Masaya Tanno

TEL:+81-11-611-2111

Fax:+81-11-644-7958

Email:tannom@sapmed.ac.jp

J Diabetes Invest 2023

ABSTRACT

Aims/Introduction: We previously showed that upregulation of myocardial AMP deaminase (AMPD) is associated with pressure overload-induced diastolic dysfunction in type 2 diabetic hearts. Here we examined involvement of AMPD localized in the ER-mitochondria interface in mitochondrial Ca²⁺ overload and its pathological significance.

Materials and Methods: We used type 2 diabetic Otsuka Long-Evans-Tokushima Fatty rats (OLETF) and non-diabetic Long-Evans-Tokushima Fatty rats (LETO) as well as AMPD3-overexpressing H9c2 cells and HEK293 cells.

Results: OLETF but not LETO showed diastolic dysfunction under the condition of phenylephrine-induced pressure overload. The levels of 90-kDa AMPD3 in outer mitochondrial membranes/ER and mitochondria-associated ER membrane (MAM) fractions were significantly higher in OLETF than in LETO. The area of the MAM quantified by electron microscopic analysis was 57% larger, mitochondrial Ca²⁺ level under the condition of pressure overload was 47% higher and Ca²⁺ retention capacity in MAM-containing crude mitochondria isolated before the pressure overloading was 21% lower in OLETF than in LETO (all p values < 0.05). Transfection of FLAG-AMPD3 in cells resulted in significant enlargement of the MAM area and impairment in pyruvate/malate-driven ADP-stimulated and uncoupler-stimulated mitochondrial respiration compared to those in control cells.

Conclusions: The findings suggest that 90-kDa AMPD3 localized in the ER-mitochondria interface promotes formation of the MAM, inducing mitochondrial Ca²⁺ overload and dysfunction in type 2 diabetic hearts.

INTRODUCTION

A plethora of evidence has shown that structural, biochemical and metabolic changes are induced by diabetes and that the changes contribute to the development of diabetic cardiomyopathy^{1,2}. Although inhibitors of sodium glucose cotransporter (SGLT) 2 have been demonstrated to reduce the aggravation of heart failure in patients with type 2 diabetes, SGLT2 inhibitors have been reported to be effective for heart failure independent of the presence or absence of diabetes³. Thus, no specific therapy is currently available for diabetic cardiomyopathy.

We recently reported that upregulation of AMP deaminase (AMPD) activity in the left ventricular (LV) myocardium contributes to impairment of diastolic function under the condition of pressure overload in type 2 diabetic hearts via decreases in the level of ATP⁴⁻⁶. AMPD has been reported to be present in a full-length form and an N-terminus-truncated short form⁷⁻¹³. Enzyme activity of N-truncated AMPD3 has been reported to be only 15% of that of full-length AMPD3⁸. We previously showed that the rat myocardium expresses 90-kDa full-length AMPD3 and 78-kDa N-truncated AMPD3 and that the protein level of only 90-kDa AMPD3 was significantly elevated in

OLETF compared to that in LETO⁶. AMPD may play distinct roles depending on the subcellular compartment in which it resides. For example, we previously reported that cytosolic AMPD promoted xanthine oxidoreductase-mediated ROS production⁴, whereas AMPD3 localized in the vicinity of the ER⁶ may suppress AMP-mediated activation of glycogen phosphorylase¹⁴ and reduce glycolytic ATP.

The ER and mitochondria structurally and functionally interact at the mitochondria-associated ER membrane (MAM), where the two organelles reciprocally regulate their functions¹⁵. It has been reported that the MAM allows Ca²⁺ transport from the ER to the mitochondria via a protein bridge consisting of inositol triphosphate receptor 2 (IP3R2) on the ER and voltage-dependent anion channel (VDAC) on the outer mitochondrial membrane (OMM), both of which are linked by the molecular chaperone glucose-regulated protein (GRP) 75. Recent evidence has indicated that the MAM plays a role in the pathophysiology of diabetic cardiomyopathy¹⁶. Wu et al. reported that Fundc1, an OMM protein that binds to IP3R2¹⁷, promoted MAM formation by inhibiting proteasomal degradation of IP3R2 in type 1 diabetic hearts¹⁶. The augmented MAM formation resulted in elevation of mitochondrial Ca²⁺, thereby inducing mitochondrial fragmentation and dysfunction¹⁶. Suppression of ER-mitochondria interaction protected cardiomyocytes from hypoxia-reoxygenation injury through reduction of mitochondrial Ca²⁺ overload¹⁸, suggesting the involvement of MAM-mediated excessive mitochondrial Ca²⁺ transport in opening of the mitochondrial permeability transition pore (mPTP), a trigger of cell death^{19,20}. Dysregulation of the mPTP is also involved in mitochondrial swelling, membrane depolarization and accumulation of defective mitochondria, phenotypes observed in failing hearts²¹⁻²³.

In the present study, we tested a hypothesis that MAM-mediated mitochondrial Ca²⁺ transport is augmented by AMPD3, resulting in opening of the mPTP, mitochondrial dysfunction and diastolic dysfunction under the condition of pressure overload in type 2 diabetic hearts. The rationale for the hypothesis is as follows. In addition to the above-mentioned increase in MAM formation and mitochondrial Ca²⁺ level in type 1 diabetic hearts, we previously showed that (a) AMPD3 is significantly upregulated in Otsuka Long-Evans-Tokushima Fatty rats (OLETF), an established model of type 2 diabetes^{24,25} compared to that in non-diabetic Long Evans Tokushima-Otsuka rats (LETO)⁴⁻⁶, (b) AMPD3 is localized in the vicinity of the ER and its expression level is also higher in OLETF than in LETO⁶ and (c) the threshold for mPTP opening upon myocardial ischemia/reperfusion is reduced in type 2 diabetic hearts^{25,26}.

MATERIALS AND METHODS

Detailed methods are provided in the online supporting information (Supplementary materials and methods).

Isolation of the MAM fraction

Isolation of the MAM fraction from the heart and cells was performed following published protocols²⁷. Briefly, tissues were manually homogenized on ice. Nuclei and unbroken cells were pelleted by centrifugation. The supernatant was collected and centrifuged to separate crude mitochondria from microsome and membrane fractions. After two washes, the crude mitochondrial fraction was suspended in mitochondrial re-suspension buffer (MRB, 250 mM mannitol, 5 mM HEPES, pH 7.4, and 0.5 mM EGTA), layered on top of 30% percoll medium (225 mM mannitol, 25 mM HEPES, pH 7.4, 1 mM EGTA), and centrifuged at 95,000 g for 30 min. The MAM fraction was extracted from the percoll gradient and further purified by centrifugation to remove contaminated mitochondria. Likewise, the pure mitochondria fraction was collected from the percoll gradient and centrifuged to obtain pellets.

RESULTS

Hemodynamic responses to pressure overload

We first performed pressure-volume loop analysis using OLETF and LETO and confirmed that OLETF at the age of 35-42 weeks show phenotypes of pressure overload-induced diastolic dysfunction, a hallmark of early diabetic cardiomyopathy, as reported previously⁴⁻⁶ (Figure S1).

Subcellular distribution of AMPD3 and expression levels of AMPD3 in each subcellular fraction

Next, the subcellular distribution of AMPD3 was analyzed using homogenates of the LV myocardium of LETO (Figure 1a). We obtained the cytosolic fraction, crude mitochondrial fraction containing whole mitochondria and the mitochondria-associated ER membrane (MAM), purified mitochondrial fraction, MAM fraction and ER/ OMM fraction. The 90-kDa full-length and 78-kDa N-terminus-truncated forms of AMPD3 were detected and 90-kDa AMPD3 was predominantly observed in the whole cell fraction. The cytosolic fraction and the ER/OMM fraction showed exclusive localization of 90-kDa AMPD3, whereas 90-kDa AMPD3 and 78-kDa AMPD3 were similarly distributed in the MAM and the crude mitochondrial fraction (Figure 1a). On the other hand, in the purified mitochondrial fraction, 90-kDa AMPD3 was negligibly detected. We next examined whether expression levels of AMPD3 in the subcellular compartments are modified in type 2 diabetic hearts. Expression levels of 90-kDa AMPD3 in the whole cell, cytosol and ER-mitochondria interface, i.e., the MAM and the ER/OMM fractions, were significantly higher in OLETF than in LETO, though the expression levels in the purified mitochondrial fractions were similar in OLETF and LETO (Figure 1b,c). In contrast, expression levels of 78-kDa AMPD3 were comparable in OLETF and LETO in all of the subcellular compartments (Figure 1b,c). These findings suggests that upregulation of 90-kDa AMPD3 in the ER-mitochondria interface might be involved in the impaired hemodynamic responses to pressure overload in OLETF.

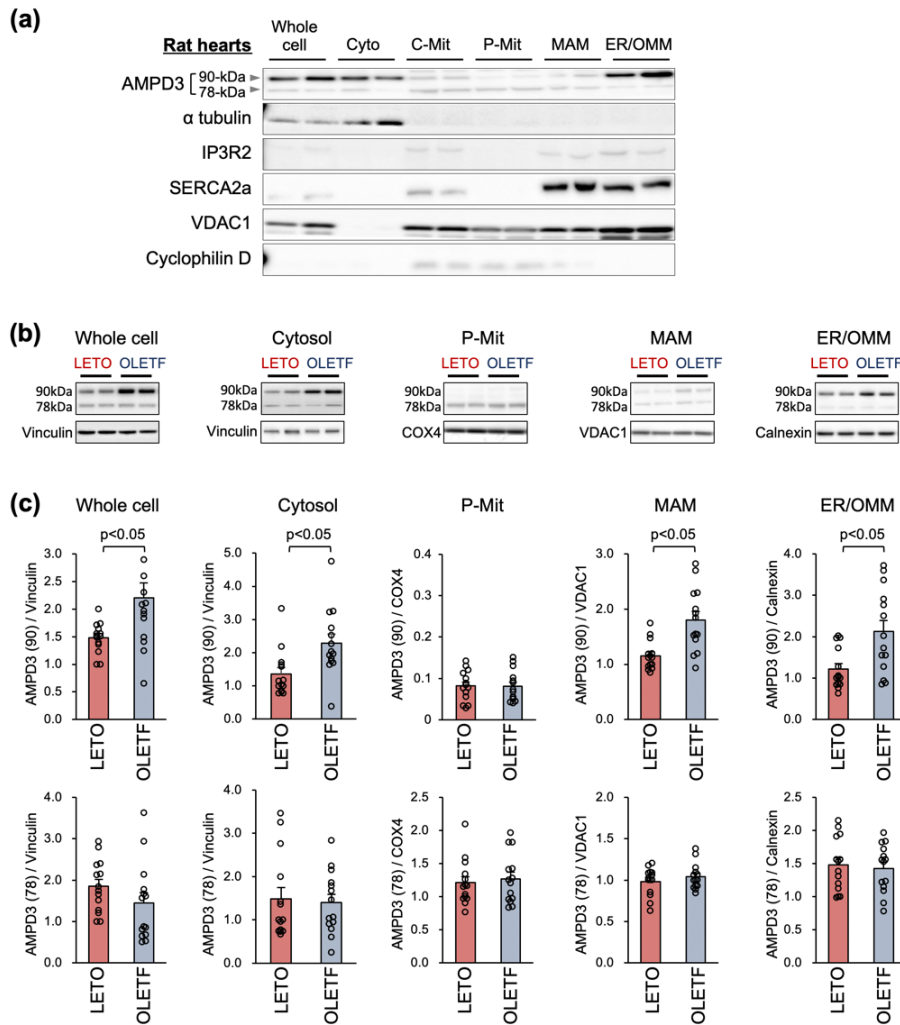


Figure 1 | Subcellular distribution of AMPD3 and expression level of AMPD3 in each subcellular fraction. (a) Representative immunoblotting for AMPD3, α tubulin, IP3R2, SERCA2a, VDAC and cyclophilin D in whole cell lysates, cytosolic fraction, crude mitochondrial fraction, purified mitochondrial fraction, MAM fraction and ER/OMM fraction in LV homogenates of LETO. (b) Representative immunoblotting for AMPD3 in whole cell, cytosol, purified mitochondria, MAM and ER/OMM fractions in LV homogenates of LETO and OLETF. (c) Densitometric analyses for protein levels of 90-kDa AMPD3 and 78-kDa AMPD3 normalized by their loading controls. Vinculin, VDAC1, Calnexin and COX4 served as loading controls. Cyto, cytosolic fraction. C-Mit, crude mitochondrial fraction. P-Mit, purified mitochondrial fraction. MAM, mitochondria-associated ER membrane fraction. ER/OMM, endoplasmic reticulum and outer mitochondrial membrane fraction. COX4, Cytochrome c oxidase subunit 4.

Quantification of the MAM area and mitochondrial Ca^{2+}

We next examined whether formation of the MAM is augmented in type 2 diabetic hearts. Areas of the MAM (Figure 2a, red arrows) quantified by measurements of MAM perimeter/ER perimeter and MAM perimeter/mitochondria perimeter were significantly larger in OLETF than in LETO (both $p < 0.05$, Figure 2b). These findings suggest that type 2 diabetes promotes formation of the MAM in the rat myocardium, in which 90-kDa AMPD3 is accumulated (Figure 1b,c). Since the MAM mediates Ca^{2+} transport from the ER to the mitochondria²⁸⁻³⁰, excessive formation of the MAM may induce mitochondrial Ca^{2+} overload. Thus, we next analyzed the mitochondrial Ca^{2+} level in the LV myocardium of OLETF and LETO with or without phenylephrine-induced pressure overloading. Under

the baseline condition, mitochondrial Ca^{2+} levels were comparable in LETO and OLETF (Figure 2c). The mitochondrial Ca^{2+} levels were significantly elevated in response to the pressure overloading both in LETO and OLETF, with OLETF showing a considerably higher mitochondrial Ca^{2+} level than that in LETO (Figure 2c). However, the expression levels of IP3R1, IP3R2, VDAC and GRP75 were comparable in LETO and OLETF (Figure 2d). Furthermore, mitochondrial Ca^{2+} uniporter (MCU), its regulatory subunits MICU1 and MICU2³¹, and Na^+ - Ca^{2+} exchanger (NCX) were also expressed at similar levels in OLETF and LETO (Figure 2d). The findings argue against the possibility that modification of expression levels of the proteins in the MAM contributes to the mitochondrial Ca^{2+} overload in OLETF.

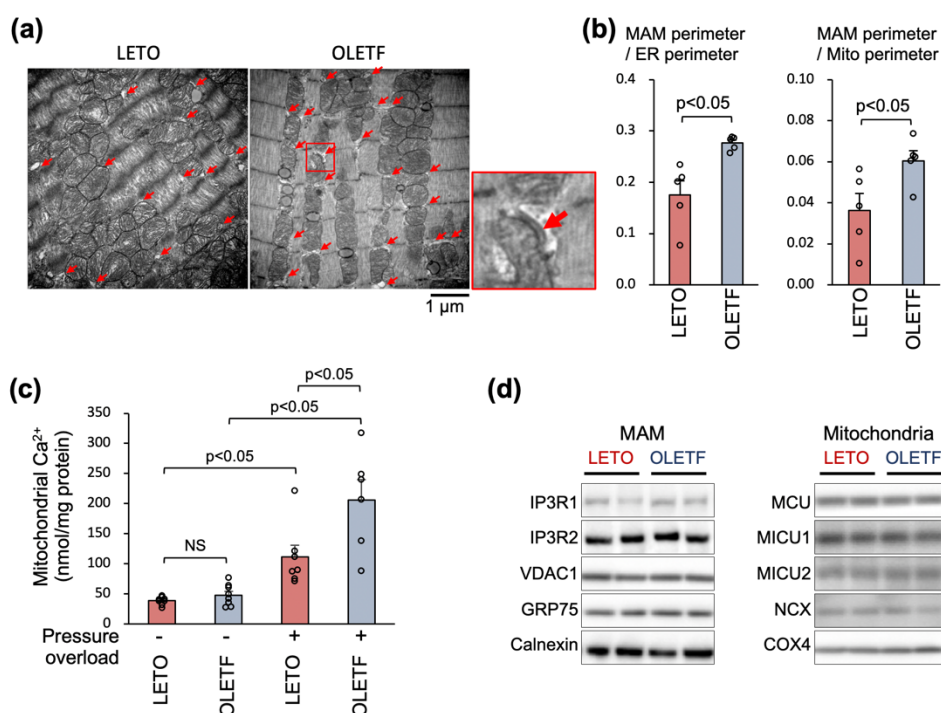


Figure 2 | Quantification of the MAM area and mitochondrial Ca^{2+} . (a) Representative electron microscopic images of LV sections in OLETF and LETO. Red arrows indicate the MAM as defined in the methods section. An enlarged image of the red squared area in OLETF is shown on the right. (b) Quantitative analyses of the MAM area in OLETF and LETO. (c) Mitochondrial Ca^{2+} levels in OLETF and LETO with or without phenylephrine-induced pressure overload. (d) Representative immunoblotting for proteins involved in the MAM formation and mitochondrial Ca^{2+} transport. IP3R, inositol 1,4,5-trisphosphate receptor. VDAC, voltage-dependent anion channel. GRP75, glucose-regulated protein 75. MCU, mitochondrial calcium uniporter. MICU, mitochondrial calcium uptake. NCX, Na^+/Ca^{2+} exchanger. Calnexin and Cox-IV served as loading controls for the MAM and IMM, respectively.

Modification of MAM area and mitochondrial Ca^{2+} by AMPD3

To examine whether upregulated AMPD3 in OLETF plays a role in the mitochondrial Ca^{2+} overload under the condition of pressure overload, we next analyzed the mitochondrial Ca^{2+} level in HEK293 cells transfected with FLAG-tagged 90-kDa AMPD3 (FLAG-AMPD3) or FLAG-control vector (Figure S2). Mitochondrial Ca^{2+} level in HEK293 cells overexpressing AMPD3 was significantly higher than that in control cells (Figure 3a), supporting the notion that AMPD3 residing in the ER-mitochondria interface may contribute to the mitochondrial Ca^{2+} overload. Interestingly, transfection of FLAG-AMPD3 significantly enlarged the area of the MAM by 36.5% compared to that with transfection of the FLAG-control (Figure 3b,c), indicating that AMPD3 is also involved in the formation of the MAM.

Modification of mitochondrial calcium retention capacity by AMPD3

Next, calcium retention capacity (CRC) was analyzed in MAM-containing crude mitochondria harvested from the LV myocardium of OLETF and LETO at baseline. As shown in Figure 4a, the Ca^{2+} level that was increased after a bolus administration of Ca^{2+} (thin arrows) was promptly decreased by uptake of Ca^{2+} into mitochondria until the

mPTP opened (bold arrow). CRC, which was defined as the total amount of Ca^{2+} administered before opening of the mPTP, was significantly lower in OLETF than in LETO (Figure 4b), indicating that either Ca^{2+} uptake through the MAM was enhanced or the threshold for mitochondrial Ca^{2+} level to trigger mPTP opening was lowered in OLETF. We previously showed that oxidative stress was significantly increased in the myocardium of OLETF compared to that in the myocardium of LETO under the condition of pressure overload⁴. However, tissue levels of 4-HNE immunoreactivity and levels of carbonylated proteins were similar in OLETF and LETO at baseline (Figure S3a,b), making it unlikely that increased oxidative stress was responsible for the reduction of CRC in OLETF in the present study. Because we previously showed that non-phosphorylated glycogen synthase kinase 3 β (GSK-3 β) reduces the threshold for mPTP opening and that ser9-phospho GSK-3 β elevates the threshold for mPTP opening^{19,32-34}, we examined the phosphorylation status of GSK-3 β in the MAM of the LV myocardium in OLETF and LETO. The ratio of ser9-phospho-GSK-3 β /non-phospho-GSK-3 β was significantly reduced in OLETF compared to that in LETO (Figure S4a,b). This finding indicates the possibility that the reduction of the threshold for mPTP opening mediated by a decrease in ser9-phospho-GSK-3 β

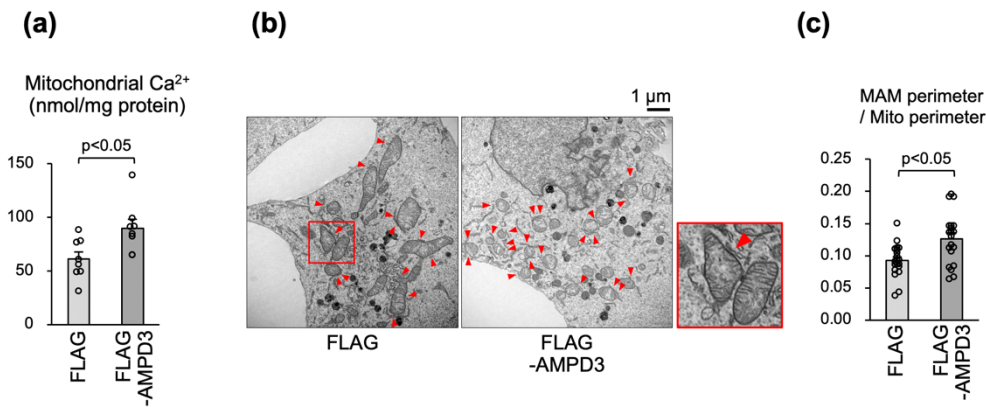


Figure 3 | Quantification of mitochondrial Ca²⁺ and the MAM area in HEK293 cells. (a) Mitochondrial Ca²⁺ levels in HEK293 cells transfected with the FLAG-control or FLAG-AMPD3. (b) Representative electron microscopic images of cells transfected with the FLAG-control or FLAG-AMPD3. Red arrowheads indicate the MAM as defined in the methods section. An enlarged image of the red squared area in cells transfected with the FLAG control is shown on the right. (c) Quantitative analyses of the MAM area.

and/or increase in non-phospho-GSK-3 β in the MAM contributed, at least partially, to the reduction of the CRC in OLETF. On the other hand, the protein levels of cyclophilin D, another crucial regulator of the mPTP²⁰, were similar in OLETF and LETO (Figure S4a,b).

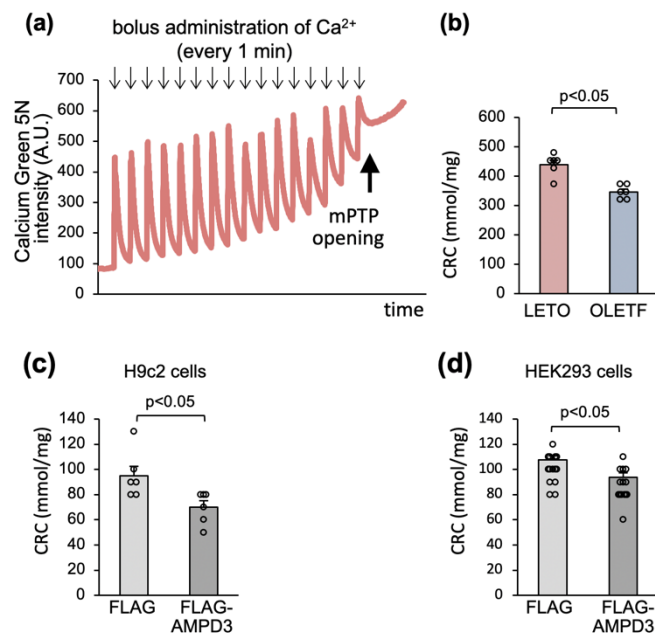


Figure 4 | Mitochondrial calcium retention capacity. (a) A representative trace to determine Ca²⁺ retention capacity (CRC) of mitochondria isolated from LETO. A bolus of 10 μ M Ca²⁺ was added to the buffer every 1 min and extracellular Ca²⁺ level was continuously monitored. Ca²⁺ level elevated by a Ca²⁺ bolus declined with uptake of Ca²⁺ into mitochondria until the mPTP opened (arrow). (b-d) Quantitative analyses of CRC in MAM-containing crude mitochondria isolated from OLETF and LETO, digitonin-permeabilized H9c2 cells and MAM-containing crude mitochondria isolated from HEK293 cells transfected with the FLAG-control or FLAG-AMPD3. mPTP, mitochondrial permeability transition pore.

To determine whether AMPD3 is directly involved in the modification of CRC, the effect of AMPD3 overexpression on CRC was analyzed in H9c2 cells and HEK293 cells. CRC was significantly lower in both digitonin-permeabilized H9c2 cells and MAM-containing crude mitochondria isolated from HEK293 cells transfected with FLAG-AMPD3 than in cells transfected with the FLAG-control (Figure 4c,d), indicating that AMPD3 in the ER-mitochondria interface plays a role in the reduction of CRC by promoting Ca²⁺ uptake through the MAM. Transfection of FLAG-AMPD3 did not affect the level of non-phosphorylated GSK-3 β , ser9-phospho-GSK-3 β or cyclophilin D (Figure S4c), excluding the possibility that 90-kDa AMPD3 modified CRC by regulating the phosphorylation status of GSK-3 β or cyclophilin D. Involvement of AMPD3 in regulation of the mPTP was further confirmed by the findings that overexpression or knockdown of AMPD3 in H9c2 cells (Figure S5) modifies oxidative stress-induced loss of mitochondrial membrane potential (Figure S6).

Modification of the function of the mitochondrial respiratory chain by AMPD3.

To elucidate the role of AMPD3 localized in the ER-mitochondria interface in mitochondrial respiration, we isolated mitochondria from HEK293 cells transfected with FLAG-AMPD3 or FLAG-control and analyzed mitochondrial respiration using an XFe96 extracellular flux analyzer. When pyruvate and malate were used as substrates to drive complex I-dependent electron transport, ADP-stimulated state 3 respiration was significantly lower by 32 % in the mitochondria isolated from AMPD3-overexpressing cells than in those isolated from control cells, whereas levels of ADP-limited state 4 respiration were comparable (Figure 5a,b). The maximal respiration induced by the addition of mitochondrial uncoupler FCCP was also significantly lower by 48% in the mitochondria of AMPD3-overexpressing cells than in those of control cells (Figure 5a,b), suggesting that decreased mitochondrial respiration in AMPD3-overexpressing cells is

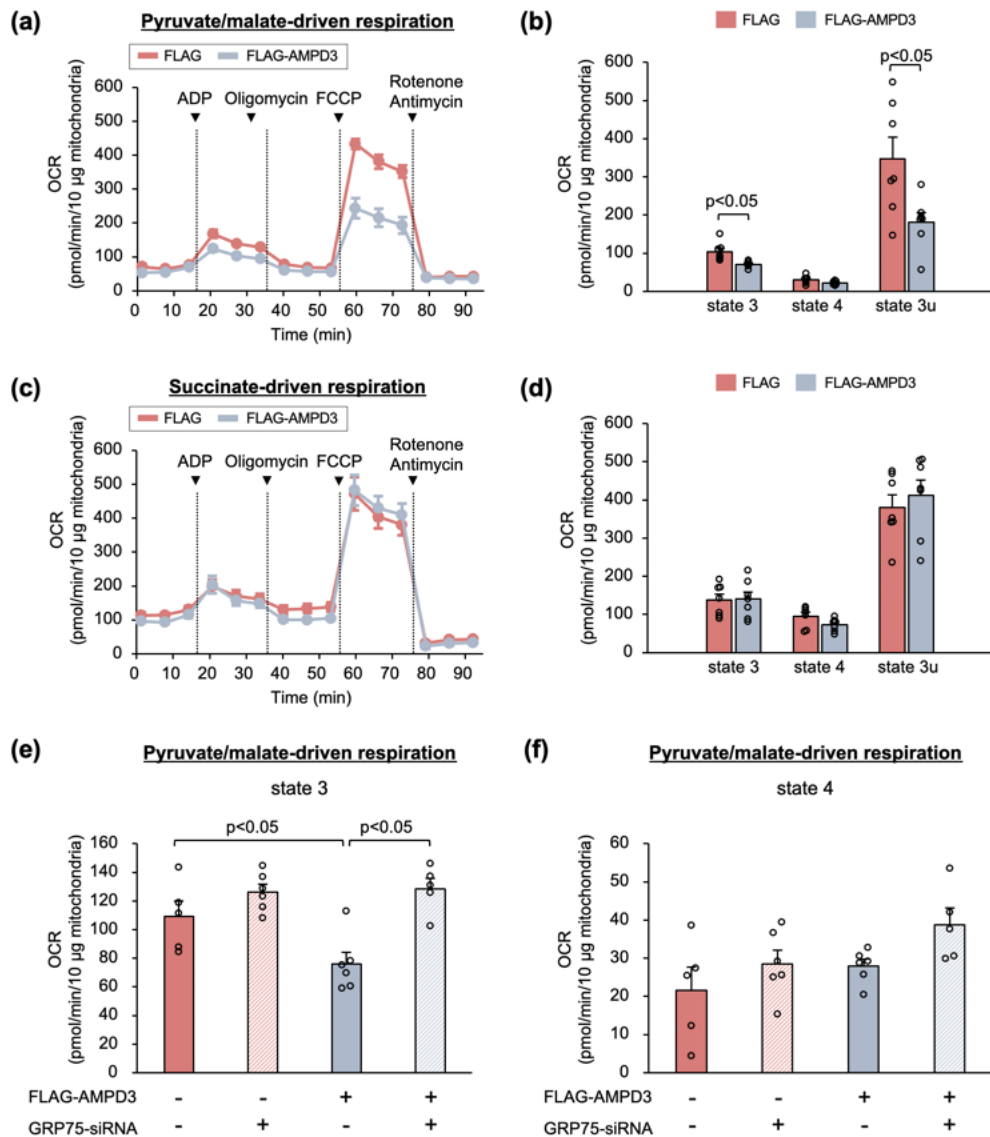


Figure 5 | Effects of overexpression of 90-kDa AMPD3 on respiratory chain function. Pyruvate/malate-driven oxygen consumption rate (OCR) determined by the Seahorse XFe96 analyzer and (b) quantitative analysis of state 3, state 4 and state 3u respiration. (c) Succinate-driven OCR determined by the Seahorse XFe96 analyzer and (d) quantitative analysis of state 3, state 4 and state 3u respiration. (e) Quantitative analysis of pyruvate/malate-driven state 3 (e) and state 4 (f) respiration. Mitochondria were isolated from HEK293 cells transfected with the FLAG-control, FLAG-AMPD3, control siRNA and/or GRP75-siRNA as described in the methods section. State 3 respiration indicates oxygen consumption with ADP, state 4 indicates respiration with oligomycin, and state 3u indicates uncoupled respiration with carbonylcyanide-4-trifluorometh-oxyphenylhydrazine (FCCP).

independent of F1F0-ATP synthase activity. On the other hand, when succinate plus rotenone were used as substrates to drive complex II-dependent electron transport, overexpression of AMPD3 did not affect state 3, state 4 or maximal respiration (Figure 5c,d). Finally, we examined whether suppression of MAM formation restores mitochondrial respiratory function in AMPD3-overexpressing cells. As a tool to reduce MAM formation, we took advantage of siRNA-mediated knockdown of GRP75, which has been reported to reduce MAM formation without affecting mitochondrial number or cell viability³⁵. Transfection of AMPD3-overexpressing HEK293 cells with GRP75-siRNA suppressed the expression of GRP75 protein by 66%, inhibited the AMPD3-mediated increase in MAM formation (Figure S7) and improved ADP-stimulated state 3 respiration but not ADP-limited state 4 respiration (Figure 5e,f). Taken together, these results suggest that AMPD3 plays a role in impairment of mitochondrial electron transport capability through complex I but not complex II by promoting MAM formation.

DISCUSSION

The results of the present study showed that both 90-kDa AMPD3 and 78-kDa AMPD3 are distributed in diverse subcellular compartments in rat hearts. The cytosolic fraction and the ER/OMM fraction showed exclusively dominant localization of 90-kDa AMPD3, whereas 90-kDa AMPD3 and 78-kDa AMPD3 were similarly distributed in the MAM and the crude mitochondrial fraction. On the other hand, the expression level of 90-kDa AMPD3 was negligible in the purified mitochondrial fraction. The 90-kDa AMPD3 levels in the ER-mitochondria interface (the MAM fraction and ER/OMM fraction), were significantly higher and the area of the MAM was significantly larger in OLETF than in LETO. The upregulated 90-kDa AMPD3 was associated with enlargement of the MAM area, mitochondrial Ca²⁺ overload, reduction in CRC and impaired mitochondrial electron transport capability through respiratory complex I.

As for the physiological significance of increased MAM area, it may be an adaptive mechanism to compensate for reduced SERCA2a

activity in type 2 diabetic hearts under unstimulated conditions. In studies using different diabetic animal models, a decrease in SERCA2a activity and impaired Ca²⁺ handling were consistently observed^{1,36}. For example, cardiomyocytes isolated from db/db mice showed decreased SERCA2a activity with a 33% delay in removal of cytosolic Ca²⁺ compared to that in non-diabetic mice³⁷. We also found that SERCA2a protein level was reduced in OLETF via ER stress-dependent augmentation of proteasomal degradation of the protein³⁸, though upregulated AMPD3 in OLETF is unlikely to mediate either reduction of SERCA2a or upregulation of ER stress (Figure S8). When Ca²⁺ uptake by SERCA2a is impaired in diabetic hearts, the Ca²⁺ store in the ER is reduced³⁶. It has been reported that ER-mitochondria Ca²⁺ transfer was suppressed under the condition in which the ER Ca²⁺ store was reduced by approximately 40%^{39,40}, indicating that ER Ca²⁺ store level affects MAM-mediated mitochondrial Ca²⁺ transport. Because the activities of some enzymes in the TCA cycle and electron transport chain depend on Ca²⁺, insufficient Ca²⁺ transfer from the ER to the mitochondria possibly perturbs physiological bioenergetics⁴¹. The enlargement of the MAM area by AMPD3 in diabetic hearts may be an adaptive change to increase the ER-mitochondria Ca²⁺ transport, restoring mitochondrial Ca²⁺ level that is requisite for maintaining mitochondrial ATP production. However, such a compensatory mechanism could become maladaptive under the condition of pressure overload, as indicated by a steeper increase of mitochondrial Ca²⁺ in OLETF than in LETO (Figure 2c).

The mechanisms underlying the increased MAM formation in type 2 diabetic hearts were not elucidated in the present study. In type 1 diabetic hearts, it has been reported that attenuated AMPK activity elevated the expression level of Fundc1. The upregulated Fundc1 augments MAM formation by binding to IP3R, thereby inhibiting proteasomal degradation of IP3R¹⁶. However, the same mechanisms are unlikely to operate in type 2 diabetic hearts, because we found that the protein level of IP3R2 was not upregulated in the LV myocardium of OLETF (Figure 2d). Since transfection of FLAG-AMPD3 resulted in significant enlargement of the MAM area in HEK293 cells (Figure 3b,c), AMPD3 should be involved in formation of the MAM. Thus, we examined the possibility that upregulated AMPD3 modifies the physical linkage of MAM-forming proteins by interacting with them. Indeed, tandem mass spectrometry analyses using anti-AMPD3 immunoprecipitates showed that AMPD3 may be associated with VDAC1 and VDAC2 but not with GRP75, IP3R2 or Fundc1 (Table S1). Although the probability of AMPD3 being associated with VDAC1 and VDAC2 is comparable between OLETF and LETO (Table S1), it is possible that upregulated AMPD3 in OLETF enhanced formation of the MAM by interacting with VDACs and increased its interaction affinity with GRP75 and/or IP3R2.

It remains unclear how increased mitochondrial Ca²⁺ content

during pressure overloading was associated with upregulation of AMPD3 in diabetic hearts. However, a possible mechanism can be speculated. It has been reported that AMPD forms a complex with glycogen particles, glycogenolytic enzymes and glycolytic enzymes in the vicinity of the ER⁴². Because glycogen phosphorylase is allosterically activated by AMP⁹ and AMPD reduces AMP level, AMPD may function as an allosteric inhibitor of glycogen phosphorylase in the ER/MAM. Since SERCA2a preferentially utilizes glycolysis-produced ATP in the vicinity of the ER⁴³, the resultant decrease in glycolytic ATP may impair Ca²⁺ uptake by SERCA2a in the MAM. As a consequence, transfer of ER-derived Ca²⁺ to the mitochondria is increased, providing the MCU with “hot spots” of a high concentration of Ca²⁺ to take up^{30,44,45}.

In conclusion, the results of the present study indicate that AMPD3 plays a role in the formation of MAMs and that upregulated AMPD3 localizing in the ER-mitochondria interface contributes to the mitochondrial Ca²⁺ overload and respiratory dysfunction during increased cardiac workload (Figure S9), leading to progression of diabetic cardiomyopathy.

ACKNOWLEDGMENTS

This study was supported by Grant-in-Aid for Scientific Research from Japan Society for the Promotion of Science (17K09584 and 21K08110), Tokyo, Japan. The authors declare no conflict of interest.

REFERENCES

1. Miki T, Yuda S, Kouzu H, et al. Diabetic cardiomyopathy: pathophysiology and clinical features. *Heart Fail Rev* 2013; 18: 149-166
2. Jia G, Hill MA and Sowers JR. Diabetic Cardiomyopathy: An Update of Mechanisms Contributing to This Clinical Entity. *Circ Res* 2018; 122: 624-638
3. Vaduganathan M, Docherty KF, Claggett BL, et al. SGLT-2 inhibitors in patients with heart failure: a comprehensive meta-analysis of five randomised controlled trials. *Lancet* 2022; 400: 757-767
4. Igaki Y, Tanno M, Sato T, et al. Xanthine oxidoreductase-mediated injury is amplified by upregulated AMP deaminase in type 2 diabetic rat hearts under the condition of pressure overload. *J Mol Cell Cardiol* 2021; 154: 21-31
5. Kouzu H, Miki T, Tanno M, et al. Excessive degradation of adenine nucleotides by up-regulated AMP deaminase underlies afterload-induced diastolic dysfunction in the type 2 diabetic heart. *J Mol Cell Cardiol* 2015; 80: 136-145
6. Tatekoshi Y, Tanno M, Kouzu H, et al. Translational regulation by miR-301b upregulates AMP deaminase in diabetic hearts. *J Mol Cell Cardiol* 2018; 119: 138-146
7. Coffee CJ and Kofke WA. Rat muscle 5'-adenylic acid aminohydrolase. I. Purification and subunit structure. *J Biol Chem*

- 1975; 250: 6653-6658
8. Mahnke-Zizelman DK, Tullson PC and Sabina RL. Novel aspects of tetramer assembly and N-terminal domain structure and function are revealed by recombinant expression of human AMP deaminase isoforms. *J Biol Chem* 1998; 273: 35118-35125
 9. Ogasawara N, Goto H, Yamada Y, et al. AMP deaminase isozymes in human tissues. *Biochim Biophys Acta* 1982; 714: 298-306
 10. Ogasawara N, Goto H, Yamada Y, et al. Subunit structures of AMP deaminase isozymes in rat. *Biochem Biophys Res Commun* 1977; 79: 671-676
 11. Ranieri-Raggi M and Raggi A. Effects of storage on activity and subunit structure of rabbit skeletal-muscle AMP deaminase. *Biochem J* 1980; 189: 367-368
 12. Sabina RL, Fishbein WN, Pezeshkpour G, et al. Molecular analysis of the myoadenylate deaminase deficiencies. *Neurology* 1992; 42: 170-179
 13. Stankiewicz A. AMP-deaminase from human skeletal muscle. subunit structure, amino-acid composition and metal content of the homogenous enzyme. *Int J Biochem* 1981; 13: 1177-1183
 14. Johnson LN. Glycogen phosphorylase: control by phosphorylation and allosteric effectors. *Faseb j* 1992; 6: 2274-2282
 15. Theurey P and Rieusset J. Mitochondria-Associated Membranes Response to Nutrient Availability and Role in Metabolic Diseases. *Trends Endocrinol Metab* 2017; 28: 32-45
 16. Wu S, Lu Q, Ding Y, et al. Hyperglycemia-Driven Inhibition of AMP-Activated Protein Kinase $\alpha 2$ Induces Diabetic Cardiomyopathy by Promoting Mitochondria-Associated Endoplasmic Reticulum Membranes In Vivo. *Circulation* 2019; 139: 1913-1936
 17. Wu S, Lu Q, Wang Q, et al. Binding of FUN14 Domain Containing 1 With Inositol 1,4,5-Trisphosphate Receptor in Mitochondria-Associated Endoplasmic Reticulum Membranes Maintains Mitochondrial Dynamics and Function in Hearts in Vivo. *Circulation* 2017; 136: 2248-2266
 18. Paillard M, Tubbs E, Thiebaut PA, et al. Depressing mitochondria-reticulum interactions protects cardiomyocytes from lethal hypoxia-reoxygenation injury. *Circulation* 2013; 128: 1555-1565
 19. Miura T and Tanno M. Mitochondria and GSK-3 β in cardioprotection against ischemia/reperfusion injury. *Cardiovasc Drugs Ther* 2010; 24: 255-263
 20. Miura T, Tanno M and Sato T. Mitochondrial kinase signalling pathways in myocardial protection from ischaemia/reperfusion-induced necrosis. *Cardiovasc Res* 2010; 88: 7-15
 21. Hafner AV, Dai J, Gomes AP, et al. Regulation of the mPTP by SIRT3-mediated deacetylation of CypD at lysine 166 suppresses age-related cardiac hypertrophy. *Aging (Albany NY)* 2010; 2: 914-923
 22. Kim I, Rodriguez-Enriquez S and Lemasters JJ. Selective degradation of mitochondria by mitophagy. *Arch Biochem Biophys* 2007; 462: 245-253
 23. Seidlmayer LK, Juettner VV, Kettlewell S, et al. Distinct mPTP activation mechanisms in ischaemia-reperfusion: contributions of Ca $^{2+}$, ROS, pH, and inorganic polyphosphate. *Cardiovasc Res* 2015; 106: 237-248
 24. Hotta H, Miura T, Miki T, et al. Angiotensin II type 1 receptor-mediated upregulation of calcineurin activity underlies impairment of cardioprotective signaling in diabetic hearts. *Circ Res* 2010; 106: 129-132
 25. Miki T, Miura T, Hotta H, et al. Endoplasmic reticulum stress in diabetic hearts abolishes erythropoietin-induced myocardial protection by impairment of phosphoglycogen synthase kinase-3 β -mediated suppression of mitochondrial permeability transition. *Diabetes* 2009; 58: 2863-2872
 26. Itoh T, Kouzu H, Miki T, et al. Cytoprotective regulation of the mitochondrial permeability transition pore is impaired in type 2 diabetic Goto-Kakizaki rat hearts. *J Mol Cell Cardiol* 2012; 53: 870-879
 27. Wieckowski MR, Giorgi C, Lebedzinska M, et al. Isolation of mitochondria-associated membranes and mitochondria from animal tissues and cells. *Nat Protoc* 2009; 4: 1582-1590
 28. Giorgi C, Missiroli S, Patergnani S, et al. Mitochondria-associated membranes: composition, molecular mechanisms, and physiopathological implications. *Antioxid Redox Signal* 2015; 22: 995-1019
 29. Rowland AA and Voeltz GK. Endoplasmic reticulum-mitochondria contacts: function of the junction. *Nat Rev Mol Cell Biol* 2012; 13: 607-625
 30. Szabadkai G, Bianchi K, Várnai P, et al. Chaperone-mediated coupling of endoplasmic reticulum and mitochondrial Ca $^{2+}$ channels. *J Cell Biol* 2006; 175: 901-911
 31. Kamer KJ and Mootha VK. MICU1 and MICU2 play nonredundant roles in the regulation of the mitochondrial calcium uniporter. *EMBO Rep* 2014; 15: 299-307
 32. Nishihara M, Miura T, Miki T, et al. Erythropoietin affords additional cardioprotection to preconditioned hearts by enhanced phosphorylation of glycogen synthase kinase-3 β . *Am J Physiol Heart Circ Physiol* 2006; 291: H748-755
 33. Nishihara M, Miura T, Miki T, et al. Modulation of the mitochondrial permeability transition pore complex in GSK-3 β -mediated myocardial protection. *J Mol Cell Cardiol* 2007; 43: 564-570
 34. Tanno M, Kuno A, Ishikawa S, et al. Translocation of glycogen synthase kinase-3 β (GSK-3 β), a trigger of permeability transition, is kinase activity-dependent and mediated by interaction with voltage-dependent anion channel 2 (VDAC2). *J Biol Chem* 2014; 289: 29285-29296
 35. Tiwary S, Nandwani A, Khan R, et al. GRP75 mediates

- endoplasmic reticulum-mitochondria coupling during palmitate-induced pancreatic β -cell apoptosis. *J Biol Chem* 2021; 297: 101368
36. Lai P, Nikolaev VO and De Jong KA. Understanding the Role of SERCA2a Microdomain Remodeling in Heart Failure Induced by Obesity and Type 2 Diabetes. *J Cardiovasc Dev Dis* 2022; 9
37. Belke DD, Swanson EA and Dillmann WH. Decreased sarcoplasmic reticulum activity and contractility in diabetic db/db mouse heart. *Diabetes* 2004; 53: 3201-3208
38. Takada A, Miki T, Kuno A, et al. Role of ER stress in ventricular contractile dysfunction in type 2 diabetes. *PLoS One* 2012; 7: e39893
39. Breckenridge DG, Stojanovic M, Marcellus RC, et al. Caspase cleavage product of BAP31 induces mitochondrial fission through endoplasmic reticulum calcium signals, enhancing cytochrome c release to the cytosol. *J Cell Biol* 2003; 160: 1115-1127
40. Pinton P, Ferrari D, Rapizzi E, et al. The Ca^{2+} concentration of the endoplasmic reticulum is a key determinant of ceramide-induced apoptosis: significance for the molecular mechanism of Bcl-2 action. *Embo j* 2001; 20: 2690-2701
41. Hayashi T, Rizzuto R, Hajnoczky G, et al. MAM: more than just a housekeeper. *Trends Cell Biol* 2009; 19: 81-88
42. Garduño E, Nogues M, Merino JM, et al. The content of glycogen phosphorylase and glycogen in preparations of sarcoplasmic reticulum-glycogenolytic complex is enhanced in diabetic rat skeletal muscle. *Diabetologia* 2001; 44: 1238-1246
43. Xu KY, Zweier JL and Becker LC. Functional coupling between glycolysis and sarcoplasmic reticulum Ca^{2+} transport. *Circ Res* 1995; 77: 88-97
44. De Stefani D, Bononi A, Romagnoli A, et al. VDAC1 selectively transfers apoptotic Ca^{2+} signals to mitochondria. *Cell Death Differ* 2012; 19: 267-273
45. Dorn GW, 2nd and Maack C. SR and mitochondria: calcium cross-talk between kissing cousins. *J Mol Cell Cardiol* 2013; 55: 42-49